

**PIPELINES AND LATERALLY LOADED PILES IN AN  
ELASTO-PLASTIC MEDIUM**

by

**B. Rajani<sup>1</sup> and N. Morgenstern<sup>2</sup>**

submitted for publication to Journal of Geotechnical Engineering, ASCE.

May 1991

---

<sup>1</sup> Ph. D. student, Department of Civil Engineering, University of Alberta, Edmonton, Alberta., Canada T6G 2G7

<sup>2</sup> University Professor, Department of Civil Engineering, University of Alberta, Edmonton, Alberta., Canada T6G 2G7

## Abstract

The uplift behaviour of a shallow pipeline embedded in an elasto-plastic medium is examined. An analytical solution for a beam on elasto-plastic foundation is developed and a characteristic non-dimensional load displacement and stress-displacement relationships are presented. An approximate 3-D solution is proposed that accounts for embedment and breakaway condition behind the pipeline making use of the load displacement curves developed for rigid anchors by Rowe and Davis (1982). A comparison of these results with those obtained by 3-D finite element analysis indicates that the simplified solution of a beam on elasto-plastic foundation is a practical alternative for analyzing the uplift behaviour of shallow pipelines. The approximate solution is also used to compare the behaviour of laterally loaded pile where no separation or separation is permitted as the load is monotonically increased. The results are presented in the form of non-dimensional charts that permit hand calculations and rapid verification of structural design of the pipeline and piles.

Key words: uplift behaviour of pipelines, elasto-plastic foundation, laterally loaded pile, breakaway.

## Introduction

Over the past decade several proposals have been put forward for the construction of a gas pipeline from the arctic to the southern populated areas (ASCE, 1978). These pipelines must be buried because of regulatory control. One method that has been suggested is to transport gas at below freezing temperatures and thus avoid the thawing of permafrost soils. However, this would lead to freezing of unfrozen soils in zones of shallow and discontinuous permafrost. It is to be expected that a frozen annulus will develop in a frost susceptible soil around the gas pipeline leading to significant water migration to the freezing front and the formation of ice lenses. Consequently, frost heave will be induced, thus forcing the pipeline to move upwards. The pipeline can undergo substantial straining leading to wrinkling buckles specially when the pipeline traverses a transition zone between two soils with different frost susceptibilities or between an unfrozen and already frozen soil. Ever since the chilled gas pipeline concept was proposed, the effect of frost heave on pipelines was identified as an important issue that should be addressed.

However, it is appropriate to note that similar interactions are present in a variety of situations such as that of a laterally loaded pile embedded in a stiff soil or permafrost, a pipeline subjected to fault movement, a pipeline subjected to landslide movement, etc. The significant differences between that of a pipeline and pile would be the imposed loads (prescribed displacements versus imposed loads) and the near surface effects would have to be accounted for with the shallow burial of the pipeline.

In order to understand the effects the soil-pipeline interaction and specially in the context of a frozen surrounding medium a number of aspects need to be considered. These include (i) the mechanics of frost susceptibility and frost heave which essentially is the nature of the loading process (ii) the modelling of mechanical properties of frozen ground (iii) the mechanical modelling response of the pipeline (iv) and the mechanical behaviour of the medium-pipeline response. Though each of these aspects has been well studied individually, there is a lack of proper understanding of the interaction between frozen soil and pipelines.

Frost susceptibility and frost heave have become reasonably well understood and have been studied (Penner and Ueda (1978), Nixon et al. (1981), Konrad and Morgenstern (1983, 1984)). These aspects will not be discussed further here. Certainly, though the prediction of frost heave is not an easy task it can be estimated reasonably with currently available experience and knowledge.

The mechanical behaviour of frozen soil has been studied by Sayles (1973), Sayles and Haines (1974), Sego and Morgenstern (1983) and others. It is now widely accepted that ice-rich frozen soil behaves like a creeping material. The most likely circumstances of a pipeline subjected to frost heave will be associated with primary and secondary creep phases of straining. The classical studies of Glen (1955) indicate that the flow law of ice-rich soils is that of the Norton type. The Norton creep relationship, rewritten in the generalized form as proposed by Ladanyi (1972) is:

$$[1] \quad \frac{\dot{\epsilon}}{\dot{\epsilon}_0} = \left( \frac{\sigma}{\sigma_0} \right)^n \quad \text{or} \quad \dot{\epsilon} = B\sigma^n$$

where  $\dot{\epsilon}$  is the axial strain rate,  $\sigma$  is the axial stress,  $\dot{\epsilon}_0$  and  $\sigma_0$  are proof strain rates and proof stress,  $B$  and  $n$  are creeping constants. Typically,  $n$  is about 3 (Morgenstern et al. 1980) for ice at low stresses and icy silts (McRoberts et al. 1978). In search for a dependence of  $n$  and  $B$  on temperature, Morgenstern et al. (1980) found from analyses of available creep data that ice behaves more as a linearly viscous material at temperatures close to 0<sup>o</sup> C. The constant  $B$  is found to be temperature and material dependent. Sego and Morgenstern (1983, 1985) have studied the behaviour of laboratory prepared polycrystalline ice and have indeed confirmed the applicability of the Norton-type power law. In the past, considerable attention has also been paid to the behaviour of polycrystalline ice primarily for glaciology studies as well as laboratory studies related to geotechnical problems. It provides a good material to work with since control can be exercised over its characteristics in the laboratory. Sego and Morgenstern (1985) studied the indentation problem using polycrystalline ice both experimentally and numerically using finite elements and they were able to simulate comparable behaviour.

We have seen above that the analysis of the interaction of frost heave with a pipeline is a complex problem in which many processes need to be examined for a proper understanding of the complete system. In the present work, we propose to decouple the frost heave process in the frost susceptible soil from the pipeline in the non-frost susceptible soil. This implies that we should apply an attenuated frost heave rate at the transition

zone of the two types of media rather than the free field frost heave rate (that which is usually measured in the laboratory). Presently, we assume that it can be readily approximated.

Previous attempts at solving this problem and specially that related to pipelines have been made by Nixon et al. (1983) and Selvadurai (1988). Nixon et al. (1983) simplified the problem to that of plane strain conditions and applied the free field frost heave over a predetermined section of the frost susceptible soil and studied its attenuation specifically at the interface of the frost and non-frost susceptible soils. However, the pipeline was considered as a passive component of the whole system and hence its interaction effects were not studied. Using the thermo-elastic analogy, Selvadurai (1988) analyzed the elastic behaviour of an embedded pipeline at shallow depth. As indicated previously, frozen soil hardly behaves as an elastic material and hence the application of this analysis is limited.

The motivation for studying the behaviour of a pipeline (beam) on elasto-plastic foundation is that for ice,  $n$  is found to be within the range of 3 to 4 and this is sufficiently large so as to be analogous to a rigid-plastic material ( $n \rightarrow \infty$ ). Of course, when  $n = 1$  in a Norton type relationship, then the material behaves as a linearly viscous material. It is this former aspect that is of interest because it permits us to establish bounds on the true behaviour. In this paper we present the solution for a beam on elasto-plastic foundation and an approximate 3-D solution is also proposed. These results are then compared with 3-D finite element

analyses and they indeed confirm the validity of the simplified 3-D solution.

Since the development of the solution is of a general nature in that it can be readily adapted to the analysis of a pipeline or a pile, we shall refer to either structure as a beam and the surrounding media as the foundation. Yamada (1988) reported an analysis along the same lines where the beam was of finite length and applied to the problem of bonded-joint cracking.

### **Beam embedded in an elasto-plastic foundation**

For the present analysis we assume that the beam is buried in a homogeneous and isotropic elasto-plastic medium and when subjected to uplift the beam deforms anti-symmetrically. We recognize that in fact for shallow pipelines this may not be totally valid. The elasto-plastic behaviour of the medium is represented by a bi-linear force-displacement relation as shown in Figure 2. If the elastic subgrade modulus is represented by  $k_s$ , then the foundation stiffness,  $k'_s$ , is given by  $k'_s = bk_s$ , where  $b$  is the beam width (pile or pipeline diameter). Typically, the maximum force/unit length,  $F_z$ , resistance available for sand (Trautmann et al. 1985) and for clay corresponding to the undrained state can be expressed respectively by:

$$[2a] \quad F_z = \gamma bzN_z$$

$$[2b] \quad F_z = \bar{N}_c bs_u = \bar{N}_c bc = \bar{N}_c b\sigma_y$$

where  $z$  is the depth of embedment and  $N_z$  is the dimensionless factor that depends on material properties of the sand,  $\gamma$  is the weight media density,  $s_u$  is the undrained strength (=  $c$  the cohesion for a purely cohesive material that follows Mohr-Coulomb failure criterion) and  $\bar{N}_c$  is a factor analogous to the bearing capacity factor which will be discussed in detail later. In the case of an elasto-plastic medium the undrained shear strength could be replaced by the yield strength,  $\sigma_y$ . Also, the limiting elastic displacement,  $U_z$ , is expressed as  $F_z/k'_s$ .

A consequence of the anti-symmetry mentioned earlier is that the transition point O (Figure 1) is a point of inflexion implying a stress boundary condition of zero moment. If on the other hand, we choose to look at the problem as that of a pile subjected to lateral load  $P$ , then the equivalent problem of a pipeline subjected to frost heave would be given by a prescribed displacement of  $w_o = P\beta/2k'_s$ , where  $\beta = \sqrt[4]{k'_s/4EI}$  where  $E$  and  $I$  are beam elastic modulus and moment of inertia respectively,  $\beta$  is the so called characteristic length. We also note that the resulting problem is statically indeterminate. We shall formulate the problem in terms of the load,  $P$ , but the corresponding prescribed end displacement solution can be obtained as indicated above. A sequence of events as a result of the interaction between the beam and the surrounding foundation take place as the load is monotonically increased and these can be described as follows:

- On initial application of the end load,  $P$  (load level  $P_1$ ), the embedded beam as well as the soil behave elastically.



- As the load is increased to a load level  $P_2$ , ultimate passive resistance will be developed in part of the surrounding soil media but the pipe will remain elastic. Referring to Figure 1, we define an axis x-x that distinguishes two regions: region A where the medium is in an elasto-plastic state and region B where the medium is still elastic. The position of the axis x-x will shift from initial position (s-s) where it is initially coincident with the edge where the load or prescribed displacement is applied. The shift from the far edge to the axis x-x is denoted by  $\bar{x}$  at any particular loading stage.
- as the load is further increased to, say, load level  $P_3$ , the distance  $\bar{x}$  increases until a plastic hinge begins to develop in the beam or wrinkles develop in the beam depending on the structural characteristics of the beam.

Our object here is to trace this load resistance behaviour for the first two events.

Stage  $0 \leq P \leq P_1$  and  $w \leq U_z$

As noted earlier, for a load  $0 \leq P \leq P_1$  and as long as the displacement  $w$  does not exceed the elastic displacement limit of the soil,  $w \leq U_z$ , the solution for a beam on elastic foundation is perfectly valid and the corresponding differential equation, boundary conditions and solution (Hetenyi, 1968) are:

$$[3] \quad EI \frac{d^4 w}{dx^4} + k'_s w = 0$$

and at  $x = 0$ , we have  $M = EIw'' = 0$  and  $V = EIw''' = P$  The displacement is given by:

$$[4] \quad w = \frac{2P\beta}{k'_s} e^{-\beta x} \cos \beta x$$

for  $0 \leq x \leq \infty$ .

Stage  $P_1 \leq P \leq P_2$  and  $w \geq U_z$

As soon as the beam displaces sufficiently so as to exceed the elastic displacement limit,  $U_z$ , then a maximum force resistance will be acting on that portion of the beam while the rest of beam-foundation is still elastic. The equilibrium equations for the two regions described earlier are:

$$[5] \quad \text{region A: } -\bar{x} \leq x \leq 0 \quad EI \frac{d^4 w_A}{dx^4} = -F_z$$

$$[6] \quad \text{region B: } 0 \leq x \leq \infty \quad EI \frac{d^4 w_B}{dx^4} + k'_s w_B = 0$$

where  $\bar{x}$  has been defined earlier. The corresponding solution for the differential equations are:

$$[7] \quad w_A = -\frac{F_z x^4}{24EI} + \frac{C_1 x^3}{6} + \frac{C_2 x^2}{2} + C_3 x + C_4$$

$$[8] \quad w_B = e^{-\beta x} [C_5 \cos \beta x + C_6 \sin \beta x]$$

where  $C_i$ ,  $i = 1, 2, \dots, 6$  are constants. In the above equations we have seven unknowns: six  $C_i$  constants and  $\bar{x}$ . The necessary boundary conditions are:

$$[9a] \quad \text{at } x = -\bar{x} \quad \text{for moment:} \quad -M = EIw'' = 0$$

$$\text{and shear:} \quad -S = EIw''' = P$$

for displacement and slope compatibility, and moment and shear equilibrium at  $x = 0$ , we have

$$[9b] \quad \begin{array}{ll} \text{displacement:} & w_A = w_B \\ \text{for slope} & w_A'' = w_B'' \\ \text{for moment:} & w_A''' = w_B''' \\ \text{for shear:} & w_A'''' = w_B'''' \end{array}$$

The last boundary condition is obtained from the fact that at  $x = 0$  the rate of variation of shear is equal to the maximum force/unit length. i.e.

$$[9c] \quad EI \frac{d^4 w_A}{dx^4} = EI \frac{d^4 w_B}{dx^4} = -F_z$$

The seven boundary conditions given in equations [9] permits the evaluation of the seven unknown constants. They are:

$$C_1 = (P - \bar{x}F_z)/EI$$

$$\begin{aligned}
[10] \quad C_2 &= \bar{x}(P - \bar{x}F_z/2)/EI \\
C_3 &= \beta(-2\bar{x}\beta^2 P + \bar{x}^2\beta^2 F_z - F_z)/k'_s \\
C_4 &= C_5 \\
C_5 &= F_z/k'_s \\
C_6 &= -C_2/2\beta^2 \\
\text{and} \quad \bar{x}\beta &= 2P\beta/F_z - 1
\end{aligned}$$

We note from the last equation of set [10] that the region A increases (i.e.  $\bar{x}$  increases) as P increases and that  $\bar{x}$  is zero until at least:

$$[11] \quad P \geq F_z/2\beta \quad \text{and} \quad P_c = F_z/2\beta$$

The displacement at the point of application of the load can be evaluated as a function of the applied load to determine what is commonly termed as the characteristic curve. Interestingly enough, the expression so obtained can be conveniently expressed in non-dimensional form. i.e

$$[12] \quad \bar{w} = \bar{N}_c \left( \frac{1}{2} + \frac{2}{3} \frac{\bar{P}}{\bar{N}_c} + \frac{8}{3} \frac{\bar{P}^4}{\bar{N}_c^4} \right)$$

where  $\bar{w} = wk'_s/bc$  and  $\bar{P} = P\beta/bc$ . In the design of a pipeline or a pile, we would normally be interested in the maximum bending moment or stress. The maximum bending moment in the beam depends on the load level as well on which side of the transition axis (x-x) does the maximum curvature develops. Three specific load levels are identified and expressed in non-dimensional form:

$$[13a] \quad \frac{M\beta}{P} = e^{-\beta x} \sin \beta x \quad \text{where } \beta x = \pi/4 \quad \text{and } P \leq P_e$$

$$[13b] \quad \frac{M\beta}{P} = \frac{e^{-\beta \hat{x}} \bar{N}_c}{2\bar{P}} \left[ \sin \beta \hat{x} + \left( 2 \frac{\bar{P}}{\bar{N}_c} - 1 \right) \cos \beta \hat{x} \right]$$

$$\text{where} \quad \tan \beta \hat{x} = \frac{(\bar{N}_c - \bar{P})}{\bar{P}} \quad \text{and } \bar{P} \geq 2\bar{P}_e$$

$$[13c] \quad \frac{M\beta}{P} = \frac{3}{2} \frac{\bar{P}}{\bar{N}_c} + 4 - \frac{2\bar{N}_c}{\bar{P}}$$

$$\text{where} \quad \beta \hat{x} = 1 - \frac{\bar{P}}{\bar{N}_c} \quad \text{and } \bar{P}_e \leq \bar{P} \leq 2\bar{P}_e$$

Equations [13a and 13b] correspond to the case when the maximum bending moment occurs to the right of the x-x axis and [13c] corresponds to the case when the maximum bending moment occurs to the left of the axis x-x. Nonetheless, the point ( $\hat{x}$ ) of maximum moment increases as the load is monotonically increased.

### **An approximate 3-D solution for a buried beam**

Rowe and Davis (1982) examined the undrained behaviour for vertical uplift as well as horizontal movement of a rigid thin anchor in a saturated clay. Their study was limited to 2-D plane strain conditions and they considered the influences of anchor embedment, layer depth, overburden pressure and breakaway condition or separation as well as other aspects on load displacement behaviour. The numerical solutions were obtained using finite element techniques and assuming that the soil was purely cohesive

and behaved according to the Mohr-Coulomb criterion. Additional assumptions made in their study can be referred to in the cited reference. In the case of a cohesive soil and for the specific case of undrained loading response, the cohesion is equal to the undrained shear strength. Consequently, for the analysis of the uplift behaviour of the pipeline and the laterally loaded pile the maximum resistance,  $F_z$ , can be expressed as indicated in [2b]. In the present analysis we propose to use findings of Rowe and Davis (1982) related to vertical uplift of anchors to study the uplift behaviour of pipelines while that of horizontal movement of anchors to study lateral pile behaviour. Essentially we make use of the load displacement curves (commonly referred to as characteristic curves) for vertical uplift of anchors (Figures 2 and 3) and horizontal movement of anchors where fully bonding or immediate breakaway is allowed for between the anchor and soil. The specific solutions were obtained for an anchor lying on the surface, i.e.  $h/b = 0$  and for an anchor deeply buried, i.e.  $h/b = \infty$ . These provide lower and upper bounds solutions for the uplift capacity as expressed in [2b]. For a vertical anchor and embedment ratio of  $h/b = 0$  we have the Prandtl solution and  $\bar{N}_c$  is 5.14. The corresponding  $\bar{N}_c$  value for  $h/b = \infty$  is 11.42. Rowe and Davis (1982) found in their analyses that it was particularly difficult to define failure and they proposed a definition that failure is considered to be reached when the displacement is a selected multiple of that which would have been reached had the conditions remained entirely plastic. In fact, they showed through their analysis that for  $h/b > 3$ , the value of  $\bar{N}_c$  (= 11.42) is essentially constant for a vertical anchor and its variation from 5.14 for  $h/b = 0$  is practically linear till  $h/b = 3$ . Consequently, as an approximation we propose to use equivalent bi-linear representations of the vertical and

horizontal load-displacement curves for anchors for the soil in the solution for a beam embedded in an elasto-plastic media to obtain an approximate 3-D characteristic curve for the uplift capacity of a buried beam and lateral pile load-displacement characteristic. As we shall see, this also permits us to obtain an economical solution for the beam embedded in media where separation is permitted to take place between the beam and the surrounding soil.

The characteristic curves for uplift resistance of a buried beam obtained making use of the above indicated load displacement curves are shown in Figures 4 and 5. Similarly, Figures 8 and 9 show the laterally loaded behaviour when no separation or separation is allowed. The effect of separation may be of considerable importance for the lateral behaviour of a pile, while it is believed that the pipeline-frozen soil interface could sustain adhesion and thus limit if not avoid separation. The range of non-dimensional loads and displacements specified in Figures 4 and 5 do not violate Euler-Bernoulli relation which implies that the formulation presented is valid only for small-displacements.

### **Finite Element Analysis**

The following points should be kept in mind in order to compare the finite element solutions with the proposed approximate solutions using load displacement characteristics for anchors developed by Rowe and Davis (1982):

- finite element solutions for anchors as developed by Rowe and Davis (1982) represent a plane strain condition. Meanwhile, the embedded beam (pipeline or pile) in surrounding media (frozen soil or soil) is between a plane stress and plane strain condition.
- while the load displacements curves for vertical anchors given by Rowe and Davis (1982) can be directly used for the study of uplift resistance of the pipelines, the corresponding use for the understanding the behaviour of laterally loaded pile is not so obvious. For the latter case, the uppermost part of the pile can be envisaged as an anchor that steadily grows in depth (Figure 8) as the load is increased.
- A relation between elastic modulus of the continuum and the so called foundation subgrade modulus used for the simplified problem as proposed by Vesic (1961) is given by:

$$[14] \quad k'_s = \frac{0.65E_s}{1 - \nu_s^2} \sqrt[12]{\frac{E_s b^4}{EI}}$$

### Uplift resistance of buried pipeline

In order to validate the approximate 3-D solution for a beam embedded at finite depth, a finite element model for the embedded pipe was solved. A common problem in three dimensional finite elements is that the number of degrees of freedom (i.e. number of equations to be solved) increases dramatically with discretization. This is of special significance



when non-linear analysis is being carried out. As a consequence, we found that the discretization pattern was largely governed by the number of shell elements used along the circumference for representing the tube. We also wanted to ensure that the curvature of the tube was adequately represented. Hence, a choice was made to use the 4-noded thin shell element as formulated by Bathe and Dvorkin (1986) and available in Adina (1987). In order to avoid element locking, a 2 x 2 Gauss integration rule in the r-s plane was used. The surrounding medium was represented by 8-node brick finite elements and its material properties were described by the von Mises failure criterion. The finite element discretization of 12 x 5 x 5 in the x, y, z directions is shown in Figure 7. In fact, only one half of the problem needs to be solved if we take advantage of the symmetry. This same problem was also solved using an 8-noded thin shell element and the corresponding 20-node brick element but with a coarser discretization and essentially the same results were obtained.

The finite element solution for displacement and maximum moment obtained for embedment ratio of  $h/b=1.55$  are shown in Figures 4 and 5. An embedment ratio of 1.55 was chosen based on the premise that for regulatory approval a minimum cover about 1 m is required and we envisaged a gas pipeline diameter of say, 1066 mm. We observe that the finite element solution falls within the bounds established by the approximate analytical solutions. Subsequently, the approximate solution was obtained as indicated above using a depth factor,  $\bar{N}_c$ , of 6.35. It should be emphasized that this value of  $\bar{N}_c$  was obtained by trial and error procedure and without applying any rigorous analysis such as a least square analysis. We note that though the load-displacement matches quite

well, the bending moment-displacement match is closer to that of  $h/b = \infty$  case. We should keep in mind that the stress predictions using the displacement finite element technique are known to be poor and this would be especially expected in light of the coarse discretization used for the pipeline. It can be appreciated that a variety of approximate solutions can be easily obtained by varying this depth factor that corresponds to the specific  $h/b$  ratio.

#### Laterally loaded pile with and without separation

Pollalis (1982) examined the behaviour of a laterally loaded pile allowing for separation to take place as the lateral load was increased monotonically. The soil medium was considered to be elasto-plastic but both elastic shear modulus and the undrained shear strength increased linearly with depth since such a situation is usually encountered in normally consolidated clays. The laterally loaded pile was simulated using cubic beam finite elements for the pile and solved using 3-D brick finite elements for the surrounding media. The separation was accounted for by using springs elements and details can be found in the fore-mentioned reference. The constitutive model as proposed by Kavvadas (1982) for non-linear behaviour of surrounding soil was used. However, before proceeding to compare the finite element solutions with the approximate solutions it is important to bear in mind that the solutions obtained by Pollalis (1982) consider shear strength increasing linearly with depth while the above proposed solution for a beam embedded in an elasto-plastic medium as well as the solutions for anchors obtained by Rowe and Davis (1982) are only pertinent for homogeneous media. Also, we should

keep in mind that the solutions for an embedded anchor are those corresponding to that of a plane strain situation. Here, we attempt to obtain (at least qualitatively) a solution for a complex 3-D situation using simplified 2-D solutions and no suggestion is made that the analysis is rigorous but nonetheless, it does provide insight in the mechanisms involved in the behaviour of a laterally loaded pile.

The solutions as indicated by Pollalis (1982) are expressed in terms of different non-dimensional load-displacement parameters that we have selected in the above solution. Hence, the 3-D finite element solution given by Pollalis (1982) was transformed to conform to our non-dimensional parameters. It is also important to note that since Pollalis (1982) has used a linearly varying elastic modulus with depth for the surrounding soil media and consequently, when separation is not allowed for, an immediate non-linear response is obtained. Hence, data from Pollalis (1982) was adjusted to include the initial elastic behaviour.

Figure 7 shows the 3-D normalized finite element solutions as indicated above. It indeed shows that our normalization is more consistent than that proposed by Pollalis (1982). His parameter,  $\bar{\alpha} = EI/\bar{\sigma}_D b^4$ , is brought naturally into our normalization and the response obtained is within a very narrow band. It is also evident that the response obtained by Pollalis (1982) was within a narrow range of parameters and hence to compare his results with our approximate solution an extrapolation procedure was used. In order to account for the linear variation of soil properties with depth and obtain a fair comparison between the approximate analyses and the 3-D finite element method we amplified the 3-D finite element

response by 1.5 ( this factor is based on equivalence of the strain energy for the two systems). Figure 8 shows the 3-D finite element solution as compared with the upper and lower bounds obtained using approximate analysis. The approximate solution can be seen to steadily increase from the  $h/b = 0$  case to reach a steady state solution where  $h/b$  is in the range 1 to 3. In spite of the limitations cited above, it can be observed that the approximate analysis remarkably traces the trend of the more accurate finite element solution.

The separation between the back of pile and the soil can be accounted for in an approximate manner if we use the corresponding limiting solutions for horizontal anchors as given by Rowe and Davis (1982). Though the limiting resistance depends on the particular collapse criteria used, the upper and lower resistances can be estimated to be in the range  $2c$  and  $4c$ . Figure 9 shows the comparison of the characteristic load-displacement curves obtained using the approximate solution and the 3-D finite element solution. We note that the trend of the load-resistance curve is similar to that of the lower bound ( $h/b=1$ ) case and perhaps this observation provides a rational understanding of this commonly used criterion for ignoring the resistance offered by the soil media in this region.

## **Conclusions**

A simple analytical formulation for a beam on an elastic-plastic foundation is presented. The 2-D plane stress load-displacement solutions developed by Rowe and Davis (1982) have been incorporated with the

analytical formulation to obtain an approximate 3-D solution. This approximate solution was compared with the 3-D finite element solution for a shell pipe embedded in an elasto-plastic media. We have demonstrated that the bounds established by the approximate solutions are quite adequate. The approximate solution can be fine tuned to the finite element solution using the bearing capacity factor,  $\bar{N}_c$ . We found that a value of  $\bar{N}_c = 6.35$  matches the displacements well but the match of the stresses is not all that satisfactory. The approximate solution was also used to predict the effective lateral pile head stiffness and similar trends are predicted.

## Appendix I. References

"Adina - A finite element program for automatic dynamic incremental nonlinear analysis". (1987). Report ARD 87-1, ADINA R&D, Inc., Boston. MA.

American Society of Civil Engineers, (1978). "An overview of the Alaska highway gas pipeline: The world's largest project." National Convention of the American Society of Civil Engineers in Pittsburg, Penn. vi + 130p.

Bathe, K.J. and Dvorkin, E. (1986). "A formulation of general shell elements - the use of mixed interpolation of tensorial components." *International Journal for Numerical Methods in Engineering*, 22(3), 697-722.

- Glen, J.W. (1955). "The flow law of polycrystalline ice." *Proceedings of the Royal Society*, London, 228A, 519-538.
- Kavvadas, M. (1982). "Non-linear consolidation around driven piles in clays", Sc. D. thesis, Massachusetts Institute of Technology, Department of Civil Engineering. Boston, MA.
- Konrad, J.-M. and Morgenstern, N. (1983). "Frost susceptibility of soils in terms of their segregation potential." *Permafrost: Fourth International Conference Proceedings*, Fairbanks, National Academy Science, Washington, 660-665.
- Konrad, J.-M. and Morgenstern, N. (1984). "Frost heave of chilled pipelines buried in unfrozen soils." *Canadian Geotechnical Journal*, 21, 100-115.
- Ladanyi, B. (1972). "An engineering theory of creep of frozen soils." *Canadian Geotechnical Journal*, 9, 63-80.
- McRoberts, E.C., Law, T. and Murray, T. (1978). "Creep testing on undisturbed ice-rich silt." *Proceedings of Third International Permafrost Conference*. Edmonton, 539-545.
- Morgenstern, N.R., Roggensack, W.D. and Weaver, J.S. (1980). "The behaviour of friction piles in ice and ice-rich soils." *Canadian Geotechnical Journal*, 17, 405-415.

- Nixon, J., Ellwood, J. and Slusarchuk, W. (1981). "In-situ frost heave testing using cold plates." *Proceedings of Fourth Canadian Permafrost Conference*, Calgary, NRCC No. 20124. Section 7.
- Nixon, J.F., Morgenstern, N.R. and Ressor, S.N. (1983). "Frost heave-pipeline interaction using continuum mechanics." *Canadian Geotechnical Journal*, 20, 251-261.
- Penner, E. and Ueda, T., (1978). "A soil frost susceptibility test and a basis for interpreting heaving rates." *Proceedings of Third International Permafrost Conference*. Edmonton, 722-727.
- Pollalis, S.N., (1982). "Analytical and numerical techniques for predicting the lateral stiffness of piles," Ph.D. thesis, Massachusetts Institute of Technology, Department of Civil Engineering. Boston, MA.
- Rowe, R.K. and Davis, E.H. (1982). The behaviour of anchor plates in clay, *Geotechnique*, 32(1), 9-23.
- Sayles, F.H. (1973). "Triaxial and creep tests in frozen Ottawa sands." *Proceedings of 2nd International Conference on Permafrost*, North American Contribution, Yakutsk, USSR, National Academy of Sciences, Washington, D.C., 384-391.
- Sayles, F.H. and Haines, D. (1974). "Creep of frozen silt and clay". U.S. Army Cold regions research and engineering laboratory, Hanover, NH. Technical report 252. 50p.

Sego, D.C. and Morgenstern, N., (1983). "Deformation of ice under low stresses." *Canadian Geotechnical Journal*, 20(4), 587-602.

Sego, D.C. and Morgenstern, N. (1985). "Punch indentation of polycrystalline ice." *Canadian Geotechnical Journal*, 22(2), 226-233.

Selvadurai, A.P.S. (1988). "Mechanics of soil-pipeline interaction." *Proceedings of the Annual conference of The Canadian Society for Civil Engineering*, Calgary, 3, 151-173

Trautmann, C.H., O'Rourke, T.D. and Kulhawy, F., (1985). "Uplift force-displacement response of buried pipe." *Journal of Geotechnical Engineering*, ASCE, 111(9), 1061-1076.

Vesic, A.S., (1961). "Bending of beams resting on isotropic elastic solid." *Proc. ASCE*, 87(EM2), 35-51.

Yamada, S.E. (1988). "Beam on partially yielded foundation", *Journal of Engineering Mechanics.*, ASCE, 114(3), 353-363.

## **Appendix II. Notation**

The following symbols are used in this paper:

**b** = beam width, pipeline or pile diameter



- $B$  = creep proportionality constant  
 $c$  = cohesion  
 $C_i$  = constants  
 $E$  = beam elastic modulus  
 $E_s$  = soil elastic modulus  
 $F_z$  = media resistance per unit length  
 $h$  = embedment depth  
 $I$  = beam moment of inertia  
 $k_s$  = foundation subgrade modulus  
 $M$  = bending moment  
 $P$  = non-dimensional load parameter  
 $n$  = creep exponent in Norton relation  
 $\bar{N}_c$  = bearing capacity type factor  
 $N_z$  = non-dimensional parameter for evaluating soil resistance  
 $s_u$  = undrained shear strength  
 $S$  = shear  
 $w$  = displacement in the z-direction  
 $\bar{w}$  = non-dimensional displacement parameter  
 $x$  = longitudinal coordinate axis  
 $\bar{x}$  = region in plastic state  
 $\hat{x}$  = point of maximum bending moment  
 $z$  = axis normal to x-axis  
  
 $\bar{\alpha}$  = non-dimensional parameter defined by Pollalis (1982) (=  $EI/\bar{\sigma}_D b^4$ )  
 $\dot{\epsilon}_o$  = proof strain rate  
 $\gamma$  = soil weight density

$\nu_s$  = soil Poisson's ratio

$\sigma_o$  = proof stress

$\bar{\sigma}_D$  = stress at tip of pile (used by Pollalis, 1982)

$\sigma_y$  = yield stress of surrounding media

## List of Figures

- Figure 1. Vertical uplift of pipeline.
- Figure 2. Load-displacement curves for rigid anchors - no separation.
- Figure 3. Load-displacement curves for rigid anchors - with separation.
- Figure 4. Non-dimensional load-displacement curves for a beam on elasto-plastic foundation - analytical vs 3D finite elements.
- Figure 5. Non-dimensional maximum moment-displacement curves for a beam on elasto-plastic foundation - analytical vs 3D finite elements.
- Figure 6. Finite element discretization of uplift of shallow pipeline.
- Figure 7. Non-dimensional load-displacement curves for a laterally loaded pile with and without separation - 3D finite elements (data from Pollalis, 1982).
- Figure 8. Non-dimensional load-displacement curves for a laterally loaded pile without separation.- analytical vs 3D finite elements.
- Figure 9. Non-dimensional load-displacement curves for a laterally loaded pile with separation.- analytical vs 3D finite elements.

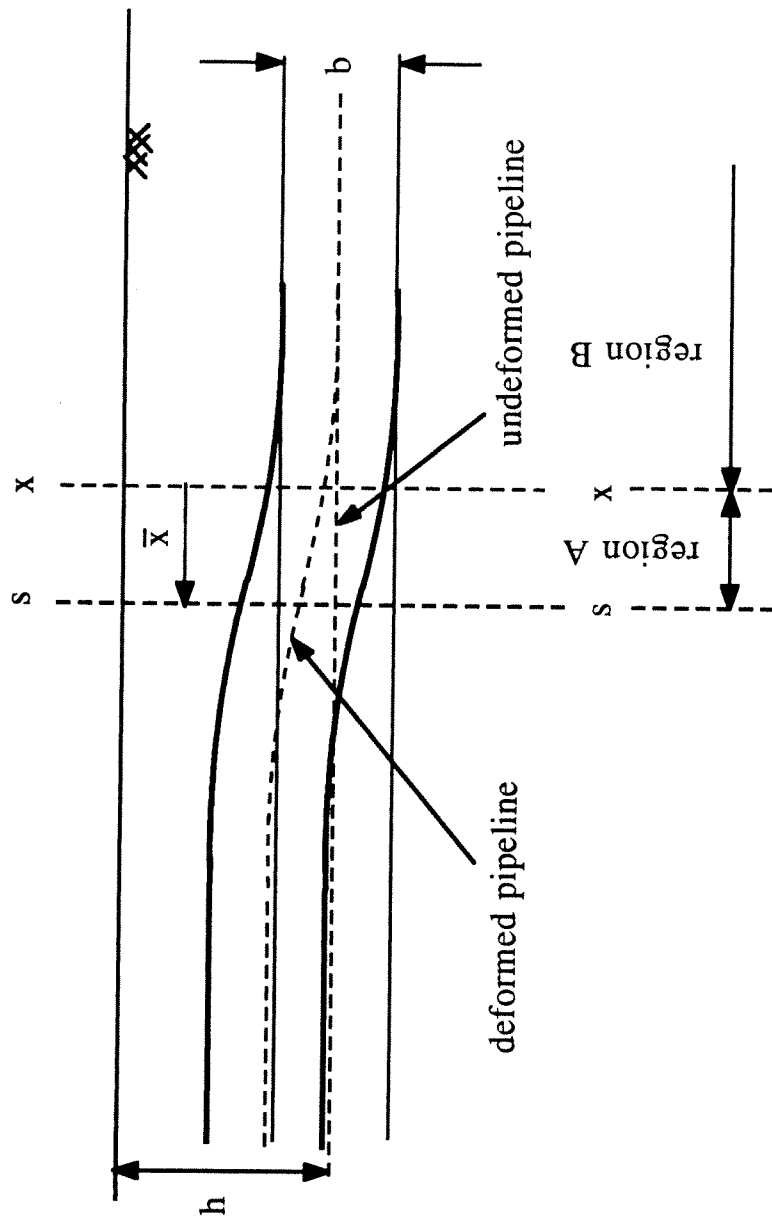


Figure 1. Vertical uplift of pipeline due to frost heave

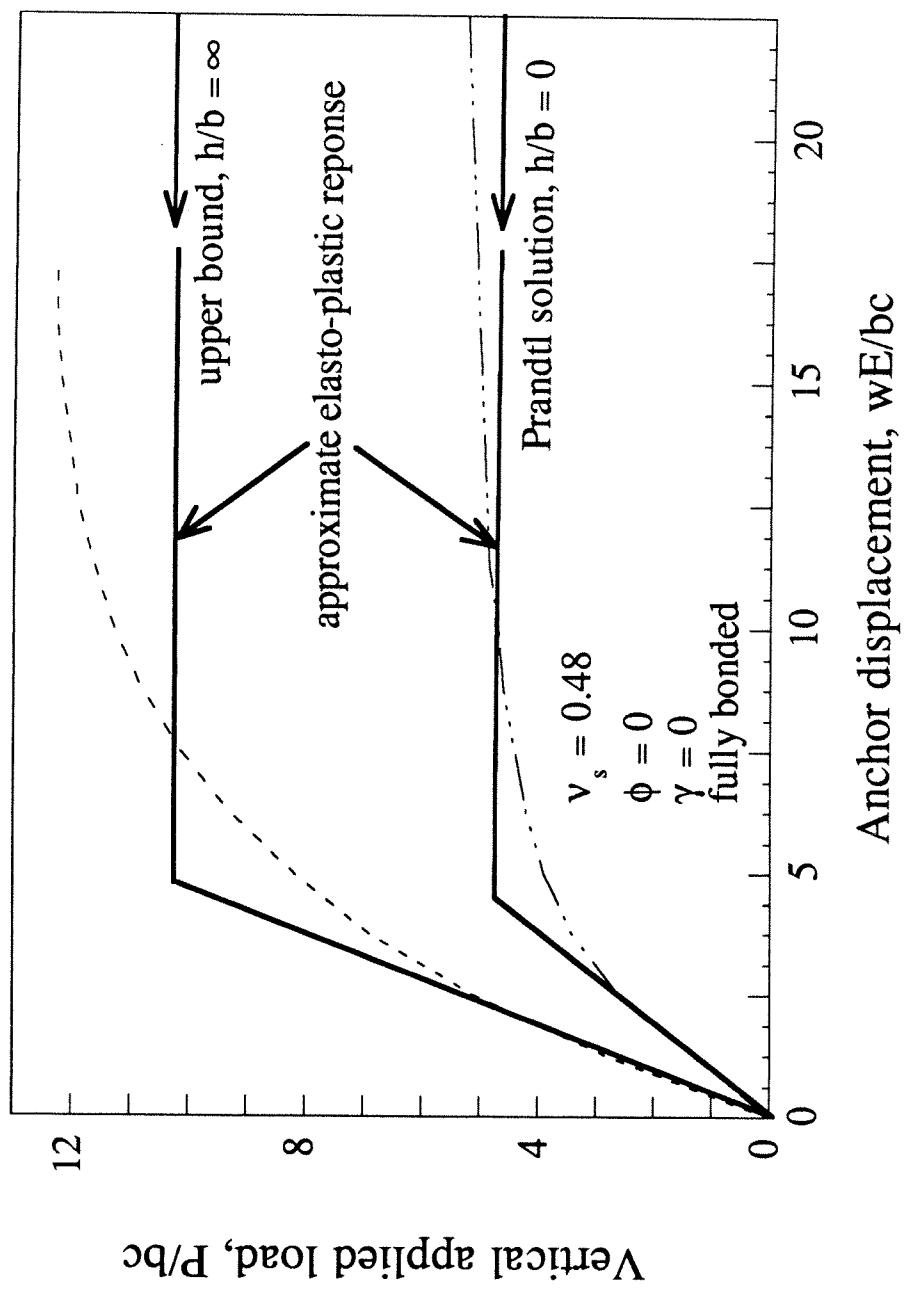


Figure 2. Load displacement curves for rigid anchors - no separation.

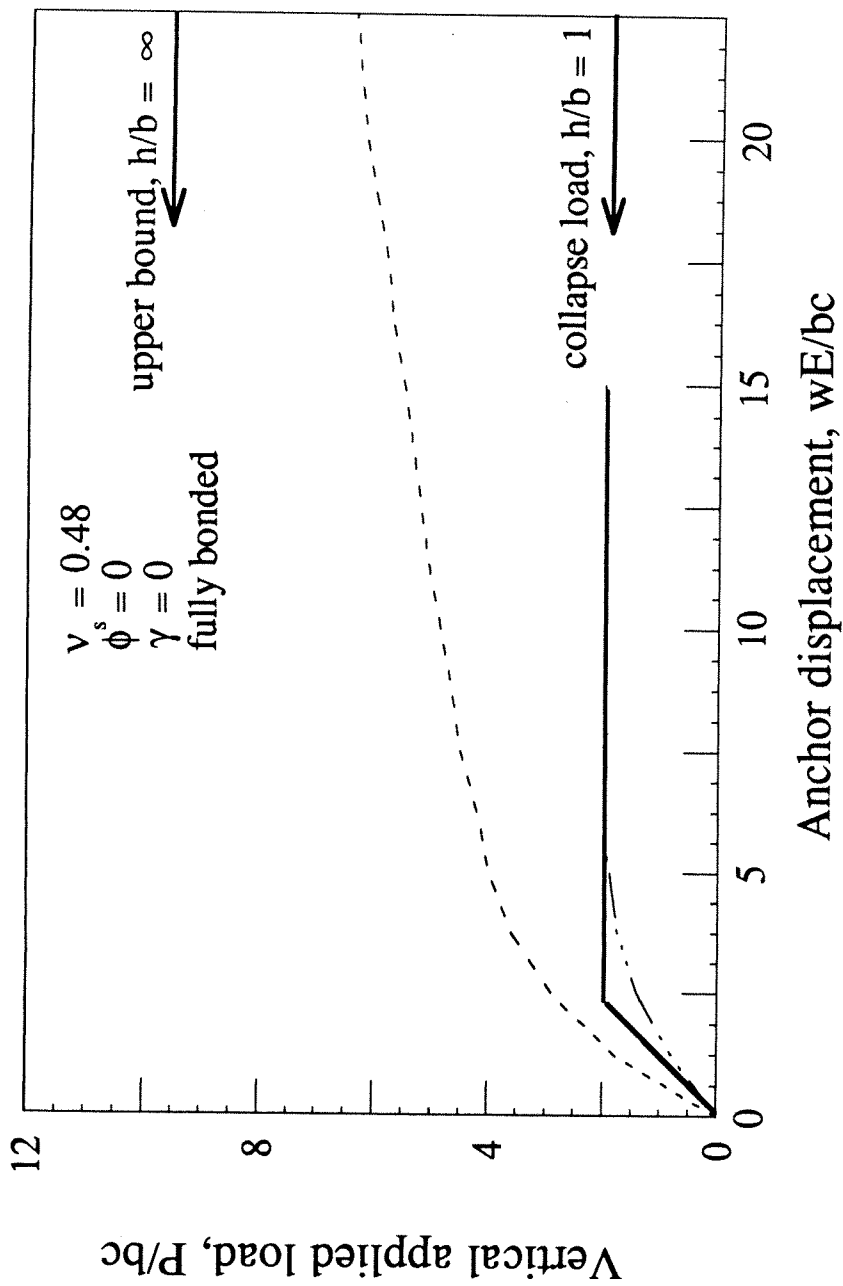


Figure 3. Load displacement curves for rigid anchors - with separation.

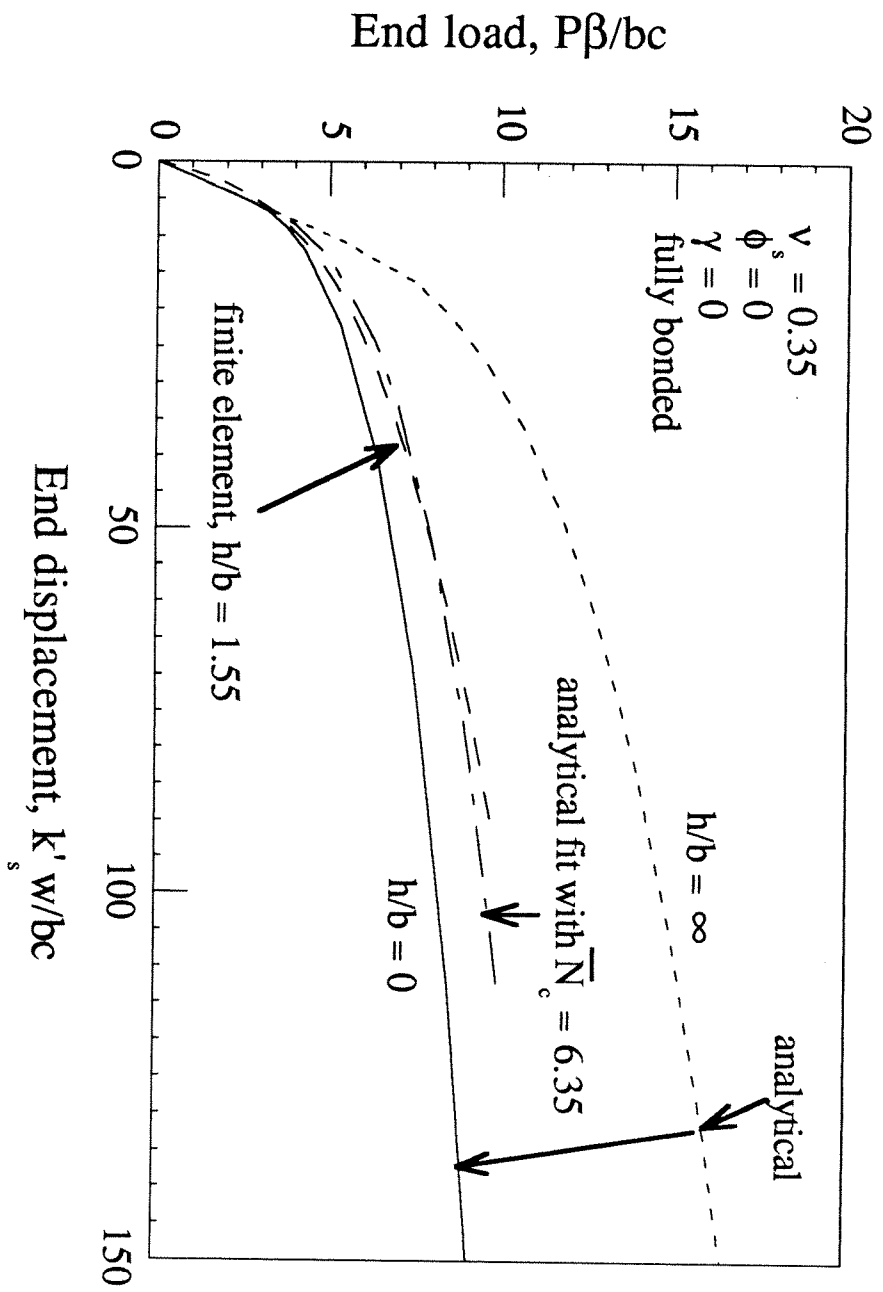


Figure 4. Non-dimensional load-displacement curve for a beam on elasto-plastic foundation - analytical vs 3D finite elements.

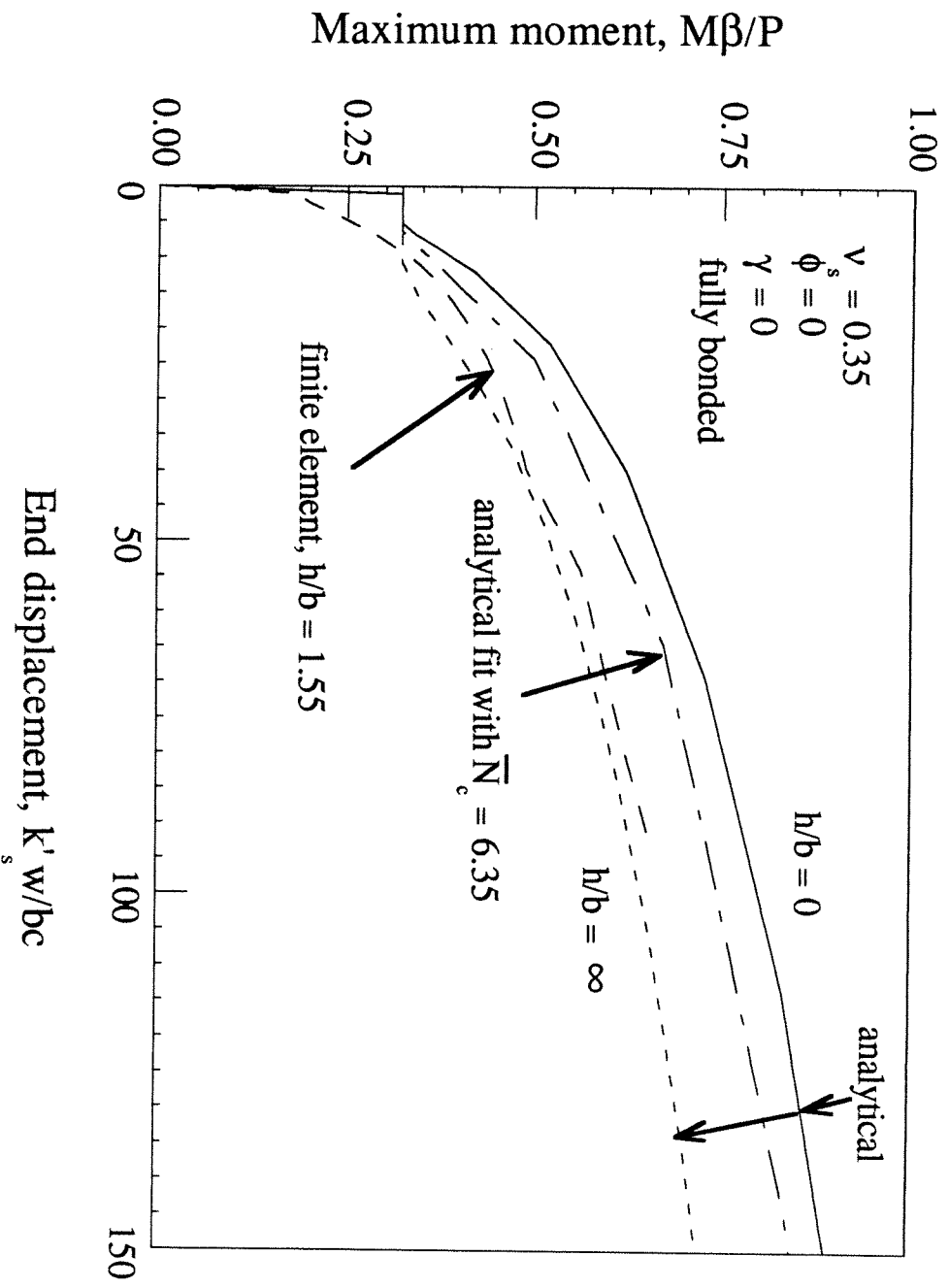


Figure 5. Non-dimensional maximum moment-displacement curve for a beam on elasto-plastic foundation - analytical vs 3D finite elements.



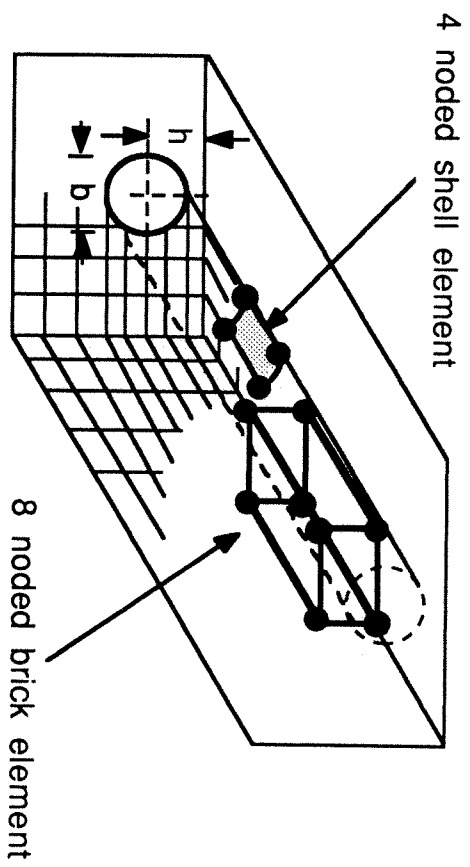


Figure 6. Finite element model for embedded pipeline

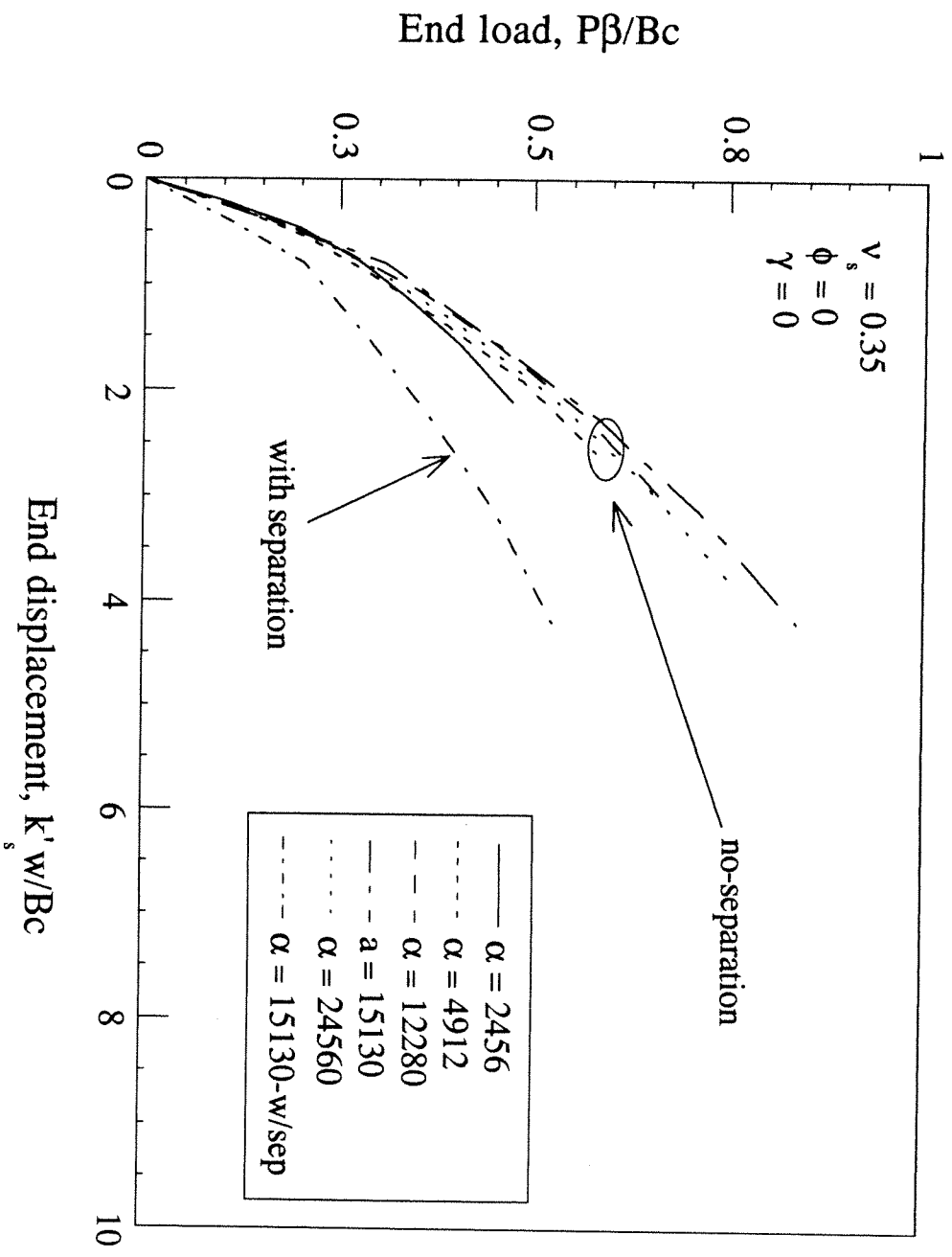


Figure 7. Non-dimensional load-displacement curve for a laterally loaded pile with and without separation - 3D finite elements (data from Pollalis, 1982).

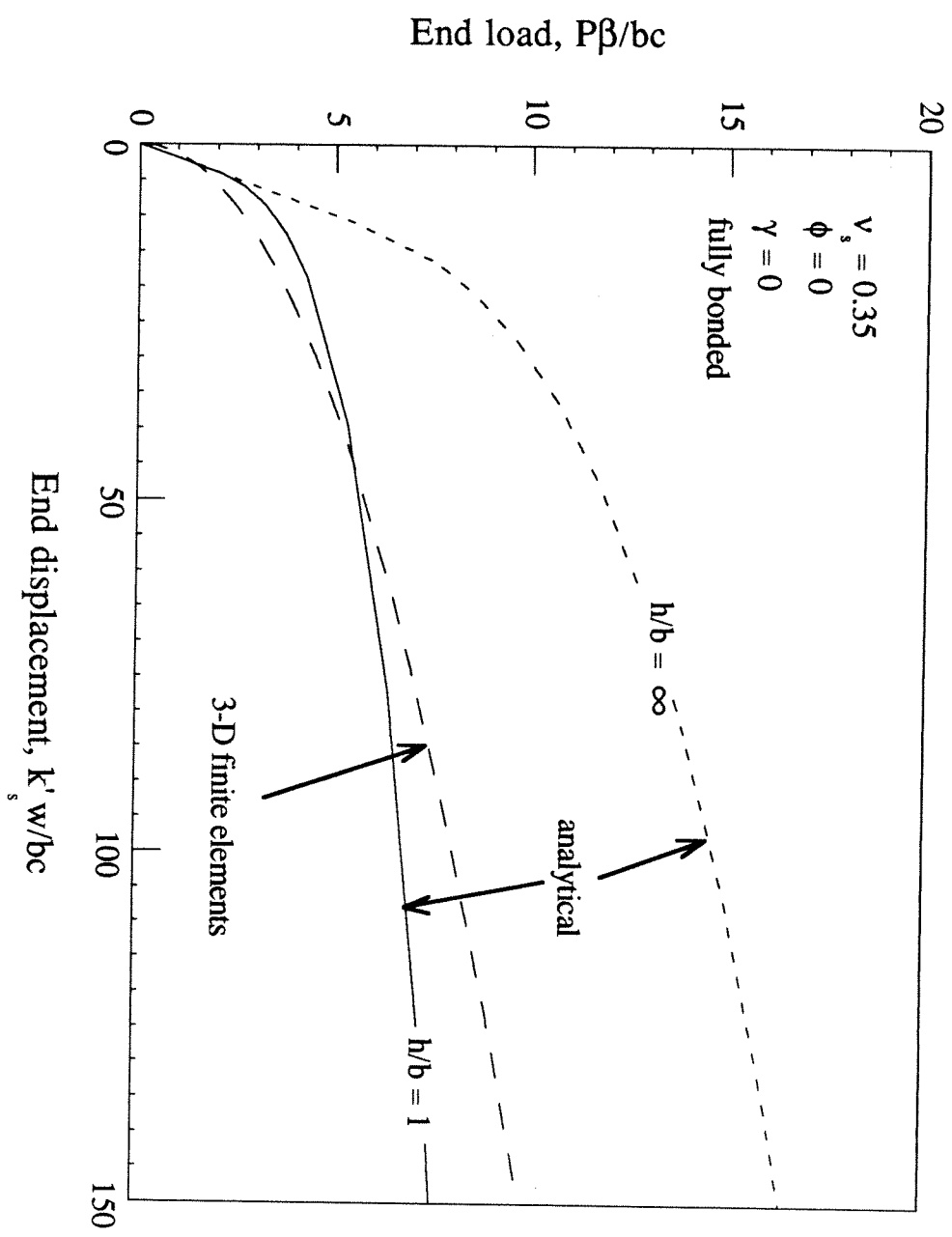


Figure 8. Non-dimensional load-displacement curve for a laterally loaded pile without separation - analytical vs 3D finite elements.

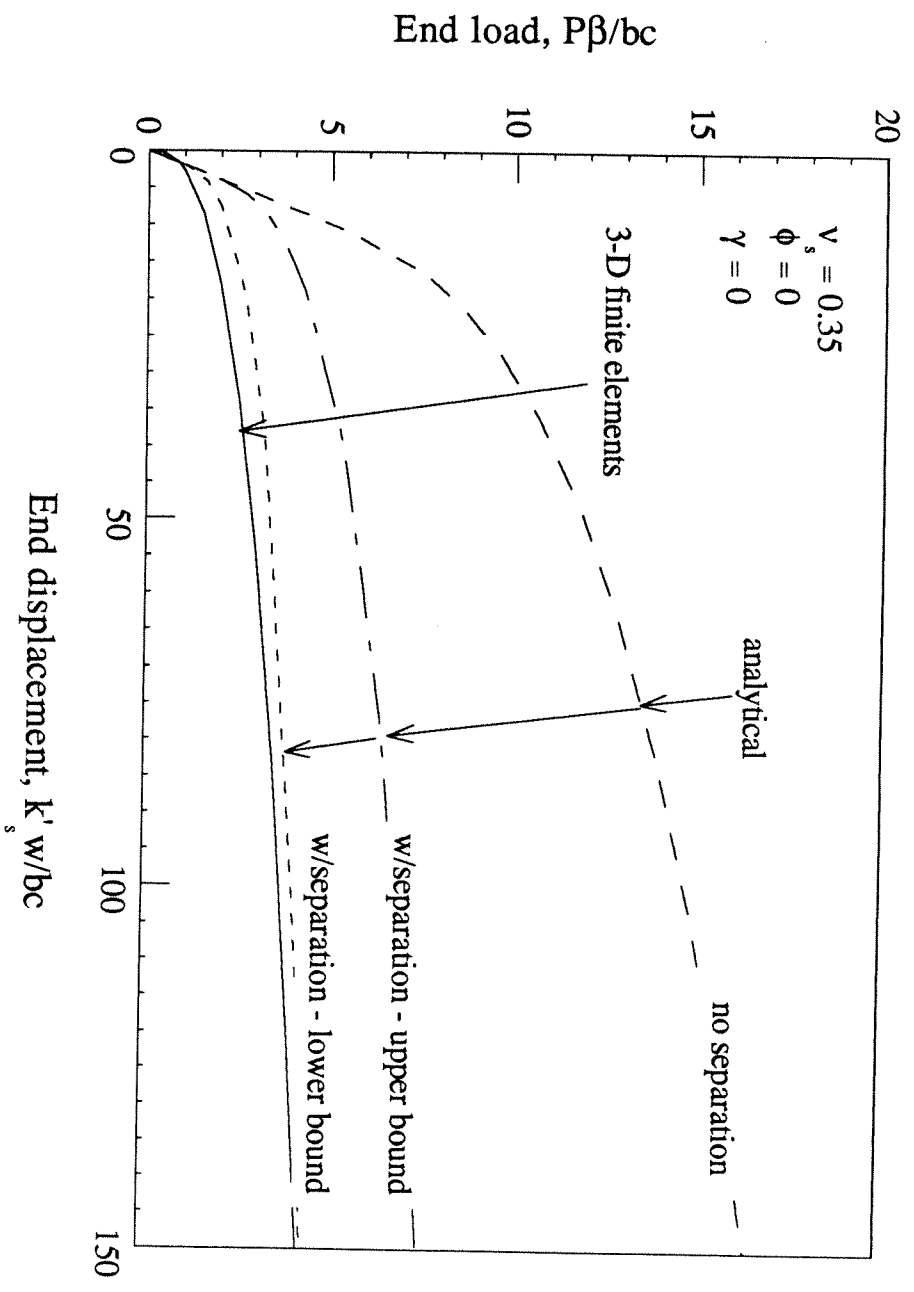


Figure 9. Non-dimensional load-displacement curve for a laterally loaded pile with separation - analytical vs 3D finite elements.